

Received December 30, 2020, accepted January 12, 2021, date of publication January 14, 2021, date of current version January 25, 2021.

Digital Object Identifier 10.1109/ACCESS.2021.3051854

# Enhanced Multiplicity on Shaped Patterns by Introducing Symmetric Pure Real Distributions: Taylor Linear and Circular Sources

AARÓN Á. SALAS-SÁNCHEZ<sup>1,2</sup>,  
J. ANTONIO RODRÍGUEZ-GONZÁLEZ<sup>1,2</sup>, (Senior Member, IEEE),  
M. ELENA LÓPEZ-MARTÍN<sup>3</sup>, AND FRANCISCO J. ARES-PENA<sup>1,2</sup>, (Fellow, IEEE)

<sup>1</sup>ELEDIA@UniTn (DISI - University of Trento), 38123 Trento, Italy

<sup>2</sup>Department of Applied Physics, CRETUS Institute, University of Santiago de Compostela, 15782 Santiago de Compostela, Spain

<sup>3</sup>Department of Morphological, CRETUS Institute, University of Santiago de Compostela, 15782 Santiago de Compostela, Spain

Corresponding author: Francisco J. Ares-Pena (francisco.ares@usc.es)

This work was supported by FEDER/Ministerio de Ciencia, Innovación y Universidades-Agencia Estatal de Investigación under Project TEC2017-86110-R. The work of Aarón Á. Salas-Sánchez was supported by the Xunta de Galicia under the Postdoctoral Fellowship under Grant ED481B 2018/008.

**ABSTRACT** The techniques on the generation of multiple solutions in shaped-beam pattern synthesis are standardly focused on the use of patterns with complex nature as input. Otherwise, in order to derive a symmetric pure real distribution from the canonical pattern synthesis techniques, a generation of a pure-real pattern has to be imposed. In the present work, the exploitation of the multiplicity of the shaped pattern generated by this symmetric pure real distribution is proposed, without constraining the solutions to necessarily meet the pure-real pattern requirement. Therefore, an increase on the degrees of freedom is produced and a greater number of continuous distributions (presenting different natures) is achieved, by omitting the restrictions found in the state-of-the-art methodologies. Thus, a general multiplicity of solutions can be reached and the design protocol can increase its number of alternatives for facing different feeding network structures. In such a way, this article is devoted to illustrate the improvements in terms of number of feasible solutions reached by the general method, including alternative symmetric pure real distributions as input within the procedure. In this manner, two different approaches, constraining the pattern to present the same number of ripples or a similar main beam width, are discussed. Examples of both Taylor distributions linear and circular are illustrated.

**INDEX TERMS** Antenna theory, aperture antennas, linear sources, planar sources.

## I. INTRODUCTION

Shaped-beam patterns have been attracting a great attention due to their advantageous performance within satellite applications. These types of desired patterns are highly interesting for guaranteeing the illumination of a controlled part of the Earth from any kind of space vehicle.

An example of numerical analysis for continuous distributions in antenna array designs can be referred [1]. In this work, the performance of reconstructing different shaped-beam patterns are analyzed. More precisely, a control of the phase distribution of the aperture for a fixed amplitude distribution has been implemented.

A very interesting feature of shaped-beam pattern synthesis is the generation of a multiplicity of solutions in terms

of continuous aperture distributions for obtaining equivalent antenna radiation patterns. In this manner, the selection of a more convenient distribution regarding practical realization and/or quality of the solution can be addressed.

Until now, among the procedures devoted to generate multiple continuous aperture distributions in shaped-beams patterns [2], [3], the idea of introducing a pure-real radiation pattern constraint has been linked to generate a unique solution in terms of aperture distribution [4], [5]. In this case, the realization of this unique solution as itself, based on a symmetric pure real continuous aperture distribution, is outlined as an advantage, because it represents the only way to obtain a distribution of such nature.

Conceptually, the generation of the multiplicity of solutions regarding continuous aperture distributions is based on phase changes of the far-field pattern and its reference level. As it is well-known [6] the phase of the far-field pattern

The associate editor coordinating the review of this manuscript and approving it for publication was Debdeep Sarkar<sup>1</sup>.

is seldom specified and this adds a degree of freedom to the work of a designer devoted to find a more realizable antenna. In such a way, an intelligent search among the different phase distributions of the pattern results in the simplest physically realizable current distribution within a specific synthesis problem. In the particular case of symmetric pure real distributions [2], [3], the inexistence of multiplicity is based on the condition of keeping a null value of this phase.

Another interesting approach is [7], where the concept of multiplicity of pure-real pattern constraints has been exploited for linear arrays. In this case, a generation of solutions based on altering the positions of the roots in the Schelkunoff unit circle representation [8] has been conducted.

Among the literature focused on power pattern synthesis problems, an interesting approach first introduced in [9] and then fully exploited in [10] can be highlighted. In these works, equivalent aperture distributions for circular patterns without deep-nulls have been obtained by means of local optimization techniques. Here, no discussion about the physical realization nor conceptual methodologies about the nature of the solutions were addressed.

In the present work, the concept of multiplicity of solutions is proposed for the pure-real pattern case (led by a symmetric pure real distribution) by eliminating the restriction in phase for the far-field pattern and allowing solutions which generate complex far-field pattern expressions. In such a way, a general methodology which completes the state-of-the-art alternatives of multiplicity and performs a comparison between the different approaches, is analyzed. More precisely, both linear and circular Taylor distributions devoted to generate equivalent pattern characteristics are considered.

For an interested reader, it is worth mentioning that, in the same basis of altering the nulls of the shaped-beam radiation patterns, alternative analytical sources could be also addressed by this procedure. For instance, shaped-beam pattern namely Rhodes [11] or Ludwig [12] distributions can be also straightforward configured as valid approaches in linear or circular sources. These patterns are generated by distributions which have been derived for going linearly to zero at the edges. Thus, they present wider beams and consequently, a reduced directivity level and aperture efficiency [13] in comparison with the Taylor case. So, the analysis of these approaches are out of the scope of this research.

**II. METHOD**

Let us consider both line and circular sources. Regarding line sources, as it is shown in the mathematical description, the methodology here proposed is also inspired in previous approaches [14] devoted to exploit asymmetrical continuous aperture distributions. At the same time, on circular sources,  $\varphi$ -symmetry will be assumed by the theoretical basis [5]. As it was above-mentioned, Taylor-based patterns have been considered in their both linear [15] and circular [16] alternatives.

**A. LINEAR SOURCES**

Let us consider a line source of length  $2l$  and centered in the origin. In such a way, the asymmetry of the aperture distribution of a shaped-beam pattern can be directly exploited from the basis of the formulation by following the general notation

$$F(u) = f(u) \cdot \prod_{n=1}^M r_{1l}(u) \cdot r_{2l}(u) \cdot r_{3l}^\epsilon(u) \cdot r_{4l}^\epsilon(u) \cdot \prod_{n=M+1}^{\bar{n}-1} \left(1 - \frac{u^2}{u_n^2}\right) \tag{1}$$

where

$$r_{il}(u) = \left(1 + (-1)^i \frac{u}{u_{in} + j\delta_{in}|v_{in}|}\right), \tag{2}$$

$u_{in} + j\delta_{in}|v_{in}|$  are the root positions and  $\delta_{in} = \pm 1$  depend on the nature of the solution,

$$f(u) = \frac{\sin(\pi u)}{\pi u} \cdot \frac{1}{\prod_{n=1}^{\bar{n}+\epsilon M-1} \left(1 - \frac{u^2}{n^2}\right)}, \tag{3}$$

where  $u = \left(\frac{2l}{\lambda}\right) \cos \theta$ , being  $\theta$  the angular direction, and  $M$  the number of filled nulls present on the pattern.

For the specific case of a pure-real pattern generated by a real symmetrical distribution,  $\epsilon = 1$  and the quadruplet of roots  $(u_{1n}, v_{1n}) = (u_n, +|v_n|)$ ,  $(u_{2n}, v_{2n}) = (u_n, +|v_n|)$ ,  $(u_{3n}, v_{3n}) = (u_n, -|v_n|)$ ,  $(u_{4n}, v_{4n}) = (u_n, -|v_n|)$ ; it is,  $\delta_n = (+1, +1, -1, -1)$  for each  $n$ .

Based on the invariance of the pattern under changes of sign in the imaginary parts of the roots ( $v_{in}$ ) a group of continuous aperture distribution can be generated, by means of the expression

$$g(\rho) = \frac{1}{2l} \sum_{m=-(\bar{n}+M-1)}^{\bar{n}+M-1} F(m) e^{jm\frac{\pi\rho}{l}}, \tag{4}$$

where  $\rho \in [-l, l]$  sweeps spatially the aperture.

This formulation permits to include both the initial complex pattern ( $\epsilon = 0$ ) and the initial pure-real pattern ( $\epsilon = 1$ ) alternatives and at the same time to generate the multiplicity of solutions by means of  $\delta = \pm 1$  in both cases.

**B. CIRCULAR SOURCES**

Regarding circular sources, a compact expression for the far-field pattern is [5]

$$F(u) = f(u) \cdot \prod_{n=1}^M r_{1c}(u) \cdot r_{2c}^\epsilon(u) \cdot \prod_{n=M+1}^{\bar{n}-1} \left(1 - \frac{u^2}{u_n^2}\right) \tag{5}$$

where  $u = \left(\frac{2a}{\lambda}\right) \sin \theta$ , being  $\theta$  the angular direction and  $a$  the radius of the distribution,

$$r_{ic}(u) = \left(1 + \frac{u^2}{(u_{in} + j\delta_{in}|v_{in}|)^2}\right), \tag{6}$$

with the root positions expressed as  $u_{in} + j\delta_{in} |v_{in}|$ , and  $\delta_{in} = \pm 1$  depending on the nature of the solution,

$$f(u) = \frac{J_1(\pi u)}{\pi u} \cdot \frac{1}{\prod_{n=1}^{\bar{n}+\epsilon M-1} \left(1 - \frac{u^2}{\gamma_{1n}^2}\right)}. \quad (7)$$

The terms  $\gamma_{1n}$  are the zeroes of the Bessel function of first kind [ $J_1(\pi \gamma_{1n}) = 0$ ].

For the particular case of a pure-real pattern generated by a pure real symmetrical distribution,  $\epsilon = 1$  and the pair of complex numbers  $(u_{1n}, v_{1n}) = (u_n, +|v_n|)$ ,  $(u_{2n}, v_{2n}) = (u_n, -|v_n|)$ ; it is,  $\delta_n = (+1, -1)$  for each  $n$ .

It is worth highlighting that the number of  $r_{ic}(u)$  terms represent the half of the  $r_{il}(u)$  terms in the linear approach and additionally they are introducing the squared value of each root. This change of procedure is motivated by the already mentioned assumption about the symmetry of the distributions.

In this case, the continuous aperture distribution which generates the far field pattern (5), (6), and (7), follows the expression [5]

$$g(\rho) = \frac{1}{2a} \sum_{m=0}^{\bar{n}+M-1} \frac{F(\gamma_{1m})}{J_0^2(\gamma_{1m}\pi)} J_0\left(\gamma_{1m} \frac{\pi \rho}{a}\right), \quad (8)$$

where  $\rho \in [0, a]$  in this case represents a radial sweep of the circular continuous aperture distribution.

### III. RESULTS

In order to analyze the proposed methodology for including a new group of solutions based on introducing initially symmetric pure real distributions, two Taylor descriptions (linear and circular) are discussed. Therefore, the synthesis of shaped-beam radiation patterns with a nominal side lobe level (SLL) of  $-25$  dB and a ripple of  $0.5$  dB will be analyzed in all the present work.

#### A. LINE SOURCES

Let us consider continuous linear distributions which generate the far-field patterns showed in Fig. 1. In particular, 3 cases are illustrated: the standard complex pattern, the input pure-real pattern constrained to present the same number of ripples than the reference (it is, 2 on each side of the shaped region) and the input pure-real pattern derived by the same number of roots than the complex pattern. In this last case, as it can be noted from Fig. 1, the generated pattern presents the half of the ripples comparing with the standard pattern. This fact is based on the reduction of the filled nulls in order to fit the requirement in terms of number of roots.

To highlight the differences between patterns, the width of the shaped region can be analyzed by means their half-power beamwidth. Regarding this parameter, while the complex pattern case presents  $26.87^\circ$ , the width for the pure-real case with the same number of ripples is of  $43.47^\circ$  (an increase of a  $61.78\%$ ). At the same time, it is worth highlighting that the alternative proposed by keeping the same number of roots presents a half-power beamwidth of  $23.35^\circ$ . This behaviour

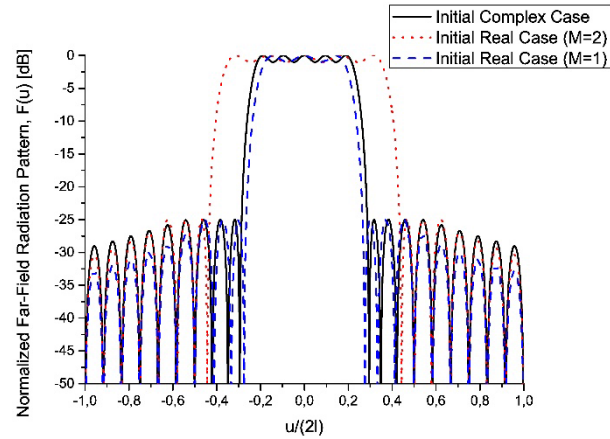


**FIGURE 1.** Results of the linear source scenario. Far-field radiation patterns of a nominal SLL of  $-25$  dB and a ripple of  $\pm 0.5$  dB: initial complex pattern with  $M = 2$  (black solid curve), initial pure-real pattern with  $M = 2$  (red dotted curve), and initial pure-real pattern with  $M = 1$  (blue dashed curve).

**TABLE 1.** Comparison of Dynamic Range Ratios  $|I_{max}|/|I_{min}|$  Between the Different Solutions in Linear Sources

Initial complex case ( $\epsilon = 0$ and $M = 2$ )			
	$ I_{max} / I_{min} $	Solution $\delta^a$	Nature
Minimum	2.51	$(+1, -1), (-1, +1)$	CS
Maximum	23.23	$(-1, -1), (+1, +1)$	RA
Initial pure-real case ( $\epsilon = 1$ ) with same number of ripples ( $M = 2$ )			
	$ I_{max} / I_{min} $	Solution $\delta^a$	Nature
Minimum	5.17	$(+1, -1, +1, -1), (-1, +1, -1, +1)$	CS
Maximum	326.88	$(-1, -1, -1, -1), (-1, -1, -1, -1)$	RA
Initial pure-real case ( $\epsilon = 1$ ) with same number of roots ( $M = 1$ )			
	$ I_{max} / I_{min} $	Solution $\delta^a$	Nature
Minimum	5.27	$(+1, -1, +1, -1), (-1, +1, -1, +1)$	CS
Maximum	44.60	$(-1, -1, -1, -1), (+1, +1, +1, +1)$	RA

<sup>a</sup>Characteristics of the solution in terms of  $\delta$  values, following (1), (2), (3), and (4).

is confirmed by analyzing the values of directivity on each case:  $16.38$  dBi for the complex pattern, while  $12.44$  dBi for the pure-real pattern of  $M = 2$ , and  $17.50$  dBi. These differences in width and directivity of the pattern motivates the inclusion of the alternative with the same number of roots, as an addition to the one devoted to generate the same pattern shape (which exactly reconstruct the same number of ripples).

Studies on the multiple solutions for the equivalent pattern generation of this linear case are reported in Table 1 by means of the analysis of the dynamic range ratio, defined as the ratio of the maximum and the minimum value of the excitation

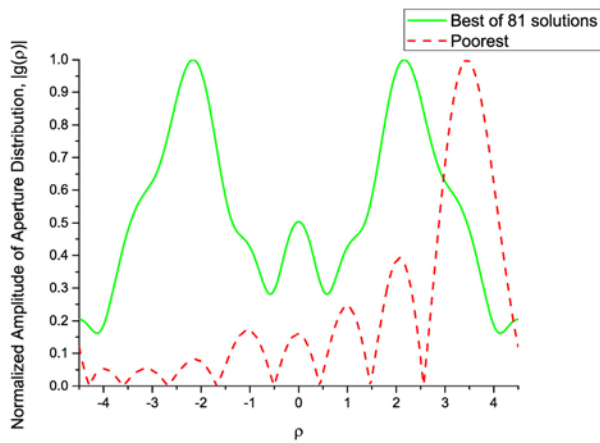


**FIGURE 2.** Comparison between the solution with minimum (green solid curve) and the solution with maximum (red dashed curve) dynamic range ratio ( $|I_{max}|/|I_{min}|$ ) of the initial pure-real case ( $\epsilon = 1$ ) with same number of ripples ( $M = 2$ ).

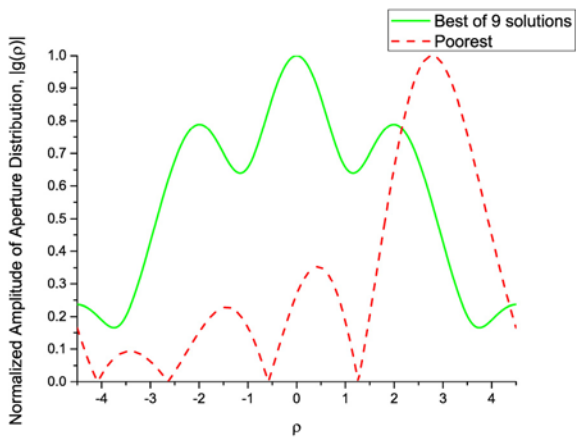


**FIGURE 3.** Comparison between the solution with minimum (green solid curve) and the solution with maximum (red dashed curve) dynamic range ratio ( $|I_{max}|/|I_{min}|$ ) of the initial pure-real case ( $\epsilon = 1$ ) with same number of roots ( $M = 1$ ).

in absolute value ( $|I_{max}|/|I_{min}|$ ). To develop this analysis, the distributions have been discretized on 19 elements with an inter-element spacing of  $0.5\lambda$ . Here, the minimum and maximum value of the dynamic range ratio for each one of the alternatives (complex and pure-real with  $M = 2$  and pure-real with  $M = 1$ ) are reported. Additionally, the shapes of the solution showing the least variation and the solution showing the greatest variation are found in Figs. 2 and 3. It is worth highlighting that the solutions with maximum variability are pure-real and they will present a change on their phases of  $180^\circ$ . In such a way, the amplitudes of the continuous distributions have necessarily to cut the axis. The greatest differences between extreme cases are the ones reported by  $M = 2$ , where minimum and maximum variability on dynamic range are 5.17 (obtained by 2 complex symmetrical solutions) and 326.88 (obtained by 2 real symmetrical solutions), respectively. At the same time, in the case of the  $M = 1$  alternative these values are 5.27 and 44.60.

Regarding practical implementation, these multiple solutions give the opportunity to the designer to select an adequate

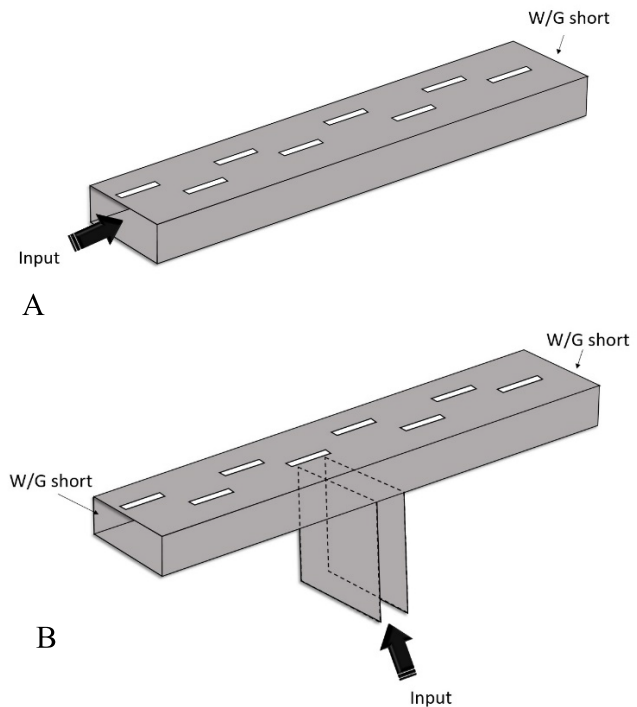


**FIGURE 4.** Illustration of different types of linear array models: A) end-fed, and B) center-fed series feed. Regarding practical realization, resonantly-spaced arrays modelled by means of these architectures will need distributions with different natures. W/G short represents a short circuit implemented at the edges of the waveguide.

nature of the continuous aperture distribution on the synthesis stage in accordance with the feeding network structure. A methodology to synthesize continuous aperture distributions can be developed by sampling at  $N + 1$  equispaced values of  $\rho$  to determine the excitation of a linear array consisting of  $N + 1$  equispaced elements [6]. In the case of the multiplicity led by the pure-real pattern with the same number of ripples, 81 solutions are derived: 1 real symmetrical, 8 real asymmetrical, 8 complex symmetrical, and 72 complex asymmetrical. On the other hand, the case of the multiplicity led by the pure-real pattern with the same number of roots represents 9 different solutions: 1 real symmetrical, 2 real asymmetrical, 2 complex symmetrical, and 4 complex asymmetrical. Thus, depending on the linear array model selected (for instance, examples of waveguide antenna designs are sketched in Fig. 4), some alternatives would be more interesting than others for discretizing the continuous distribution. More precisely, it can be highlighted that solutions involving asymmetrical aperture distributions are more interesting in the case of resonantly-spaced end-fed structures (Fig. 4.A), while symmetrical ones are of interest from the point of view of resonantly-spaced center-fed structures (Fig. 4.B). Otherwise, if the spacing of the array is  $d \neq \lambda_g/2$ , a travelling wave excitation model [6] has to be applied.

### B. CIRCULAR SOURCES

In the case of circular sources, by developing the same rationale developed for the linear problem, other 3 test cases have been analyzed. Therefore, a comparison between the

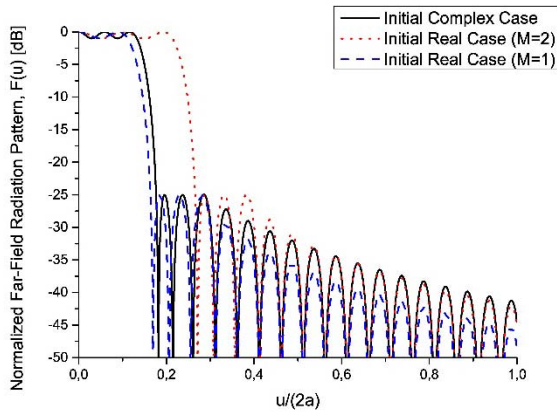


**FIGURE 5.** Results of the circular source scenario. Far-field radiation patterns of a nominal SLL of  $-25$  dB and a ripple of  $\pm 0.5$  dB: initial complex pattern with  $M = 2$  (black solid curve), initial pure-real pattern with  $M = 2$  (red dotted curve), and initial pure-real with  $M = 1$  (blue dashed curve).

standard multiplicity with  $M = 2$ , the alternative based on an initial pure-real pattern keeping the same number of ripples (with also  $M = 2$ ) and the alternative of an initial pure-real pattern keeping the same number of roots and therefore a half number of ripples ( $M = 1$ ) are reported in Fig. 5.

To highlight the differences between the effective patterns obtained by each development, the width of the shaped region is also analyzed by means of its half-power beamwidth. Regarding this parameter, while a value of  $16.48^\circ$  is obtained from the complex pattern, the width for the pure-real case with the same number of ripples is of  $26.24^\circ$  (an increase of a  $59.22\%$ ). At the same time, it is worth highlighting that the alternative proposed by keeping the same number of roots presents a half-power beamwidth of  $14.32^\circ$ . These results are in line with the values of directivity obtained for each case. They are  $23.03$  dBi for the complex pattern, while  $19.13$  dBi for the pure-real pattern of  $M = 2$ , and  $24.17$  dBi.

Studies on the multiplicity of the circular case are reported in Table 2. Here, among the analysis of the dynamic range ratio by discretizing the distributions in 20 rings with an interspacing of  $0.5\lambda$  between them, the solutions with minimum and maximum variability are highlighted. Additionally, the shapes of the best and the worst solutions of the sets are reported in Figs. 6 and 7. In the particular case of Fig. 7, a maximum variability in the solution is led by a pure-real distribution (red dashed curve). The maximum variability of this solution can be expected due to the negative region present in the function. In the same manner than for linear sources, a high level of difference between extreme cases occurs for  $M = 2$ . For these solutions, the minimum and maximum variability on dynamic range are  $13.30$  (obtained by 2 complex solutions) and  $141.79$  (obtained by pure-real solutions), respectively. At the same time, in the case of the  $M = 1$  alternative these values are  $18.29$  and  $51.92$  and their natures coincides are also complex and pure-real respectively. So, we can conclude that the pure-real solutions present a variability much higher than the complex alternatives. This issue reinforces the impact of alternatives based on producing

**TABLE 2.** Comparison of Dynamic Range Ratios  $|I_{max}|/|I_{min}|$  Between the Different Solutions in Circular Sources

Initial complex case ( $\epsilon = 0$ and $M = 2$ )			
	$ I_{max} / I_{min} $	Solution $\delta^a$	Nature
Minimum	5.81	$(+1), (-1)$ $(-1), (+1)$	C
Maximum	16.74	$(+1), (+1)$ $(-1), (-1)$	C
Initial pure-real case ( $\epsilon = 1$ ) with same number of ripples ( $M = 2$ )			
	$ I_{max} / I_{min} $	Solution $\delta^a$	Nature
Minimum	13.30	$(+1, +1), (-1, +1),$ $(-1, -1), (-1, +1)$	C
Maximum	141.79	$(+1, -1), (+1, -1)$	R
Initial pure-real case ( $\epsilon = 1$ ) with same number of roots ( $M = 1$ )			
	$ I_{max} / I_{min} $	Solution $\delta^a$	Nature
Minimum	18.29	$(+1, +1)$ $(-1, -1)$	C
Maximum	51.92	$(+1, -1)$	R

<sup>a</sup>Characteristics of the solution in terms of  $\delta$  values, following (5), (6), (7) and (8).

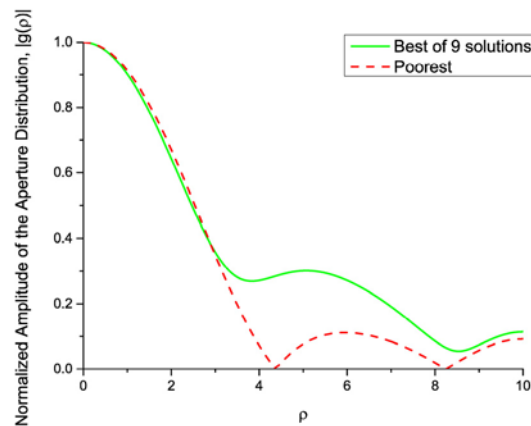


**FIGURE 6.** Comparison between the solution with minimum (green solid curve) and the solution with maximum (red dashed curve) dynamic range ratio ( $|I_{max}|/|I_{min}|$ ) of the initial pure-real case ( $\epsilon = 1$ ) with same number of ripples ( $M = 2$ ).

complex solutions within the framework of the pure-real pattern constraint, as the one here devised.

Thus, regarding practical implementation and to illustrate the importance of exploiting a new group of natures for the distribution we can analyze the sketch from Fig. 8, where a practical 2D design involving waveguide slot array antennas is depicted. This implementation can be conducted by conventional sampling the continuous distributions [6]. For instance, the theory behind the procedure to reconstruct a certain continuous distribution in order to generate a desired radiation pattern has been improved in [17].

Furthermore, an extension to conformal arrays can be performed by means of straightforward methods. For instance, in [18] a rapid synthesis of irregular footprints was proposed. In order to achieve an arbitrary footprint, it is necessary to

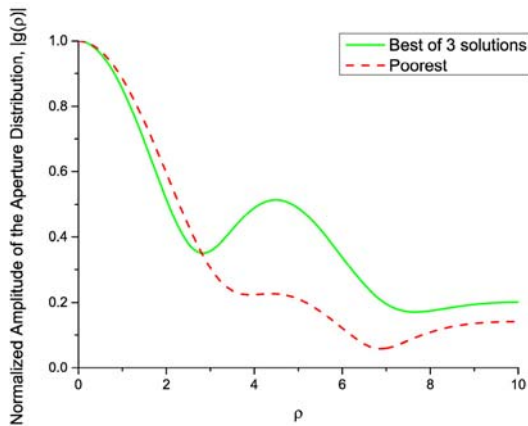


**FIGURE 7.** Comparison between the solution with minimum (green solid curve) and the solution with maximum (red dashed curve) dynamic range ratio ( $|I_{max}|/|I_{min}|$ ) of the initial pure-real case ( $\epsilon = 1$ ) with same number of roots ( $M = 1$ ).

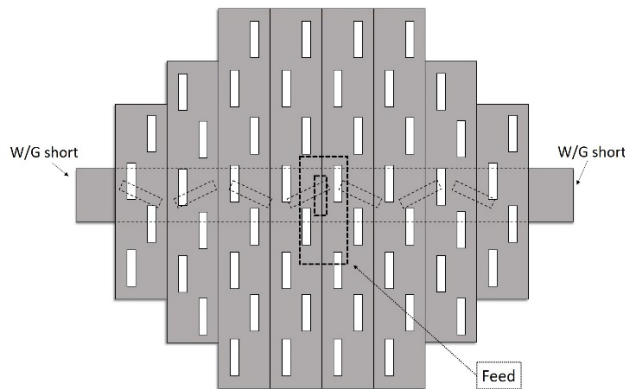


**FIGURE 8.** Illustration of a center-fed series feed planar array. Regarding practical realization, for planar waveguide slot antenna arrays with resonantly-spaced elements the unique feasible solution is the real symmetric aperture distribution. W/G short represents a short circuit implemented at the edges of the main line feed waveguide.

match the extent of the region to be illuminated on each pattern cut. This can be done by stretching or shrinking the continuous circular aperture distribution namely a radius that is inversely proportional to the desired flat-top half-power beam width (HPBW).

So, a general example of center-fed array is drawn in Fig. 8, where symmetrical circular solutions are, in general, realizable solutions. In this analysis of circular sources the initial pure-real alternative generating the same number of ripples represents an addition of 9 new distributions (1 real and 8 complex) instead of just 1 real. On the other hand, the other pure-real alternative with the same number of roots adds 3 new (1 real and 2 complex) solutions, instead of just the real one. In the particular case of resonantly-spaced planar antenna of a center fed structure (Fig. 8) just solutions with pure-real nature represent a feasible alternative.

#### IV. CONCLUSION

New alternatives concerning different natures of continuous aperture distributions in antenna pattern synthesis can be introduced for improving shaped-beam multiplicity studies.

Not only a valuable contribution to this issue is performed by the solutions which generate patterns with the same number of ripples in the shaped region, but also solutions which generate an equivalent pattern with the same number of roots reported interesting potentials. Therefore, a procedure to produce an enhanced multiplicity of solutions in the case of shaped-beam patterns has been proposed.

Additionally, as it has been illustrated in this work, the practical realization of an array according with the feeding network characteristics motivates the analysis of different types (in terms of nature) of continuous aperture distributions which generate equivalent shaped-beam patterns. To this end, simple sketches of feasible situations which can be addressed by means of the general multiplicity procedure here devised have been shown.

The inclusion of this procedure has been derived in both frameworks: linear and circular sources. By analyzing the numerical results showed in case of linear distributions, complex symmetrical solutions represent an advantage in terms of aperture variability, while the real asymmetrical alternatives represent a more extreme solution in terms of variability and therefore, they are more difficult to implement in practice. Alternatively, regarding circular aperture distributions, complex solutions represent advantages against real ones, because these last ones represent the worst alternative in terms of dynamic range ratio for generating a shaped-beam patterns.

In this manner, the multiplicity of solutions reached by the present methodology can be highlighted and interesting potentials for facing different antenna designs can be reported, since they represent an increased number of alternatives to consider. Thus, that discussion reinforces the importance of looking for new alternatives out of the state-of-the-art by means of different continuous aperture natures, in order to add more degrees of freedom for implementing a global strategy on antenna design.

#### REFERENCES

- [1] A. Trastoy-Rios, M. Vicente-Lozano, and F. Ares-Pena, "Shaped beams from circular apertures and arrays with uniform amplitude," *Electron. Lett.*, vol. 36, no. 14, pp. 1180–1182, Jul. 2000, doi: [10.1049/el:20000903](https://doi.org/10.1049/el:20000903).
- [2] F. Ares, R. S. Elliott, and E. Moreno, "Optimised synthesis of shaped line-source antenna beams," *Electron. Lett.*, vol. 29, no. 12, pp. 1136–1137, Jun. 1993, doi: [10.1049/el:19930758](https://doi.org/10.1049/el:19930758).
- [3] R. S. Elliott and G. J. Stern, "Shaped patterns from a continuous planar aperture distribution," *IEE Proc. H (Microw., Antennas Propag.)*, vol. 135, no. 6, pp. 366–370, Dec. 1993, doi: [10.1049/ip-h-2.1988.0077](https://doi.org/10.1049/ip-h-2.1988.0077).
- [4] F. Ares, R. S. Elliott, and E. Moreno, "Synthesis of shaped line-source antenna beams using pure real distributions," *Electron. Lett.*, vol. 30, no. 4, pp. 280–281, Feb. 1994, doi: [10.1049/el:19940226](https://doi.org/10.1049/el:19940226).
- [5] R. S. Elliott and G. J. Stern, "Footprint patterns obtained by planar arrays," *IEE Proc. H (Microw., Antennas Propag.)*, vol. 137, no. 2, pp. 108–112, Apr. 1990, doi: [10.1049/ip-h-2.1990.0020](https://doi.org/10.1049/ip-h-2.1990.0020).
- [6] R. S. Elliott, *Antenna Theory and Design*, Rev. ed. Piscataway, NJ, USA: IEEE Press, 2003.
- [7] A. A. Salas-Sanchez, P. Rocca, J. A. Rodriguez-Gonzalez, and F. J. Ares-Pena, "Exploiting real far field patterns into the multiplicity of solutions for linear array pattern synthesis: Bandwidth studies," in *Proc. 14th Eur. Conf. Antennas Propag. (EuCAP)*, Copenhagen, Denmark, Mar. 2020, pp. 1–5, doi: [10.23919/EuCAP48036.2020.9135566](https://doi.org/10.23919/EuCAP48036.2020.9135566).
- [8] S. A. Schelkunoff, "A mathematical theory of linear arrays," *Bell Syst. Tech. J.*, vol. 22, no. 1, pp. 80–107, Jan. 1943, doi: [10.1002/j.1538-7305.1943.tb01306.x](https://doi.org/10.1002/j.1538-7305.1943.tb01306.x).

- [9] O. M. Bucci, T. Isernia, and A. F. Morabito, "Optimal synthesis of circularly symmetric aperture sources with shaped patterns," in *Proc. 5th Eur. Conf. Antennas Propag. (EUCAP)*, Rome, Italy, Apr. 2011, pp. 1287–1290.
- [10] O. M. Bucci, T. Isernia, and A. F. Morabito, "Optimal synthesis of circularly symmetric shaped beams," *IEEE Trans. Antennas Propag.*, vol. 62, no. 4, pp. 1954–1964, Apr. 2014, doi: [10.1109/TAP.2014.2302842](https://doi.org/10.1109/TAP.2014.2302842).
- [11] J. C. Brégains, J. A. Rodríguez, F. Ares, and E. Moreno, "Optimal synthesis of line source antennas based on rhodes distributions," *Prog. Electromagn. Res.*, vol. 36, pp. 1–19, 2002, doi: [10.2528/PIER01110203](https://doi.org/10.2528/PIER01110203).
- [12] J. C. Brégains, "Optimal synthesis of circular apertures based on ludwig distributions," *Electromagnetics*, vol. 23, no. 1, pp. 41–53, Jan. 2003, doi: [10.1080/02726340390159414](https://doi.org/10.1080/02726340390159414).
- [13] *IEEE Standard for Definitions of Terms for Antennas*, IEEE Standard 145-2013 (Revision of IEEE Standard 145-1993), pp. 1–50, 6 Mar. 2014, doi: [10.1109/IEEESTD.2014.6758443](https://doi.org/10.1109/IEEESTD.2014.6758443).
- [14] J. C. Brégains, J. A. Rodríguez, F. Ares, and E. Moreno, "On the multiplicity of solutions of Taylor linear sources generating symmetrical power patterns with filled nulls [antenna design applications]," *IEEE Antennas Wireless Propag. Lett.*, vol. 3, pp. 169–171, 2004, doi: [10.1109/LAWP.2004.833708](https://doi.org/10.1109/LAWP.2004.833708).
- [15] T. T. Taylor, "Design of line-source antennas for narrow beamwidth and low side lobes," *Trans. IRE Prof. Group Antennas Propag.*, vol. 3, no. 1, pp. 16–28, Jan. 1955, doi: [10.1109/TPGAP.1955.5720407](https://doi.org/10.1109/TPGAP.1955.5720407).
- [16] T. Taylor, "Design of circular apertures for narrow beamwidth and low sidelobes," *IRE Trans. Antennas Propag.*, vol. 8, no. 1, pp. 17–22, Jan. 1960, doi: [10.1109/TAP.1960.1144807](https://doi.org/10.1109/TAP.1960.1144807).
- [17] R. E. Hodges and Y. Rahmat-Samii, "On sampling continuous aperture distributions for discrete planar arrays," *IEEE Trans. Antennas Propag.*, vol. 44, no. 11, pp. 1499–1508, Nov. 1996, doi: [10.1109/8.542075](https://doi.org/10.1109/8.542075).
- [18] J. Fondevila-Gómez, J. A. Rodríguez-González, J. Brégains, E. Moreno, and F. Ares, "Very fast method to synthesise conformal arrays," *Electron. Lett.*, vol. 43, no. 16, pp. 856–857, Aug. 2007, doi: [10.1049/el:20071543](https://doi.org/10.1049/el:20071543).



**AARÓN Á. SALAS-SÁNCHEZ** was born in A Coruña, Spain, in 1988. He received the degree in physics, the M.S. degree in engineering mathematics, and the Ph.D. degree in mathematical modeling and numerical simulation in engineering and applied science from the University of Santiago de Compostela, Spain, in 2012, 2014, and 2018, respectively.

He was a Visiting Ph.D. Student with the Department of Electrical Engineering and Information Technology, University Federico II of Naples, Italy, in 2015. He is currently a Xunta de Galicia International Postdoctoral Fellow with the Department of Applied Physics, University of Santiago de Compostela, which brings him the opportunity to be Visiting Postdoctoral Researcher in ELEDIA Research Center, University of Trento, Italy, by two years. His current research interests include numerical methods in solving electromagnetic problems and antenna array pattern synthesis.

Dr. Salas-Sánchez has been awarded the "Extraordinary Doctorate Award 2017-2018" by the University of Santiago de Compostela for the research work developed during his Ph.D. Thesis.



**J. ANTONIO RODRÍGUEZ-GONZÁLEZ** (Senior Member, IEEE) was born in Orense, Spain, in 1972. He received the B.S. and M.S. degrees in physics and the Ph.D. degree from the University of Santiago de Compostela, Spain, in 1995, 1996, and 1999, respectively.

He is currently an Associate Professor with the Department of Applied Physics, University of Santiago de Compostela. He has authored more than 200 articles for journals, conferences, and collaborative volumes. His current research interests include numerical methods for solving electromagnetic problems and pattern synthesis, computer programming, and software engineering in general.

Dr. Rodríguez-González was a Secretary of the Spanish Committee of the International Union of Radio Science (URSI), from 2011 to 2017. He received the Outstanding Ph.D. Award from Physics Faculty, University of Santiago de Compostela, in 2000, and was awarded the Teaching Innovation Prize at the University of Santiago de Compostela, in 2006.



**M. ELENA LÓPEZ-MARTÍN** was born in Segovia, Spain, in 1963. She received the Ph.D. degree in medicine from the University of Santiago de Compostela, Spain, in 1999.

She is currently an Associate Professor of human anatomy with the Morphological Sciences Department, University of Santiago de Compostela. She has authored or coauthored more than 110 articles and scientific communications. Her current research interests include the study of electromagnetic pollution, the biological effects of mobile telephony, and the therapeutic application of microwaves in the central nervous system (CNS) and peripheral tissues.

Dr. López-Martín has been the Spanish Official Member of the Commission K (Electromagnetics in Biology and Medicine) in the International Union of Radio Science (URSI), since 2014. She serves as a reviewer for different international journals, including the *Progress in Electromagnetic Research (PIER)*, *Bioelectromagnetics*, *Biomedical and Environmental Science*, *Mutation Research*, and the *International Journal of Radiation Biology*.



**FRANCISCO J. ARES-PENA** (Fellow, IEEE) received the B.S., M.S., and Ph.D. degrees in physics from the University of Santiago de Compostela, Spain, in 1986, 1987, and 1993, respectively.

He was a Research Scholar with the Department of Electrical Engineering, University of California at Los Angeles, Los Angeles, for two quarters, in 1990 and 1991, where he developed the main topic of his Ph.D. thesis. He is currently a Full Professor with the Department of Applied Physics, University of Santiago de Compostela, Spain. He has authored more than 390 articles for journals, conferences, and collaborative volumes. His current research interests include numerical methods in solving electromagnetic problems and antenna array pattern synthesis.

Dr. Ares-Pena received the Outstanding Ph.D. Award from the Physics Faculty, University of Santiago de Compostela, in 1994, and the Teaching Innovation Prize of the University of Santiago de Compostela, in 2006. He served as an Associate Editor for the IEEE TRANSACTIONS ON ANTENNAS AND PROPAGATION, from 2016 to 2019. He was the President of the Spanish Committee of the International Union of Radio Science (URSI), from 2011 to 2017.

...